BENTHAM SCIENCE

CrossMark

Current Medical Imaging

Content list available at: https://benthamscience.com/journals/cmir

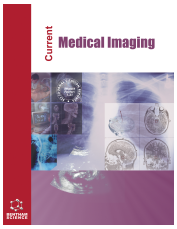

RESEARCH ARTICLE

Combination of Contrast-enhanced FlAIR and Contrast-enhanced T1WI: A Quick and Efficient Method in Detecting Brain Metastases of Lung Cancers

Linlin Sun[1,#], Shihai Luan[2,3,4,#], Xiaodan Ye[5], Jing Chen[1], Jueqian Shi[1], Huiyuan Zhu[1], Haiyang Dong[1], Guangyu Tao[1], Xuemei Liu[1], Li Zhu[1,*] and Hong Yu[1,*]

[1]*Department of Radiology, Shanghai Chest Hospital, School of Medicine, Shanghai Jiao Tong University , Shanghai, PR, China*
[2]*Department of Neurosurgery, Huashan Hospital, Fudan University, Shanghai, PR, China*
[3]*Institute of Neurosurgery, Fudan University, Shanghai, PR, China*
[4]*Shanghai Key Laboratory of Brain Function Restoration and Neural Regeneration, Fudan University, Shanghai, PR, China*
[5]*Department of Radiology, Zhongshan Hospital, Fudan University, Shanghai, PR, China*

Abstract:

Background:

Some patients with suspected brain metastases (BM) could not tolerate longer scanning examinations according to the standardized MRI protocol.

Objective:

The purpose of this study was to evaluate the clinical value of contrast-enhanced fast fluid-attenuated inversion recovery (CE FLAIR) imaging in combination with contrast-enhanced T1 weighted imaging (CE T1WI) in detecting BM of lung cancer and explore a quick and effective MRI protocol.

Material and Methods:

In 201 patients with lung cancers and suspected BM, T1WI and FLAIR were performed before and after administration of gadopentetate dimeglumine. Two radiologists reviewed pre- and post-contrast images to determine the presence of abnormal contrast enhancement or signal intensity and decided whether it was metastatic or not on CE T1WI (Group 1) and CE FLAIR (Group 2). The number, locations and features of abnormal findings in two groups were recorded. Receiver Operating Characteristic (ROC) analyses were conducted in three groups: Group 1, 2 and 3(combination of CE FLAIR and CE T1WI).

Results:

A total of 714 abnormal findings were revealed, of which 672 were considered as BM and 42 nonmetastatic. Superficial and small metastases(≤10mm) in parenchyma and ependyma, leptomeningeal and non-expansive skull metastases were typically better seen on CE FLAIR. The areas under ROC in the three groups were 0.720,0.887 and 0.973, respectively. Group 3 was significantly better in diagnostic efficiency of BMs than Group 1 ($p<0.0001$) or Group 2 ($p=0.0006$).

Conclusion:

The combination of CE T1WI and CE FLAIR promotes diagnostic performance and results in better observation and characterization of BM in patients with lung cancers. It provides a quick and efficient way of detecting BM.

Keywords: Fluid-attenuated inversion recovery imaging, T1 weighted imaging, Contrast enhancement, Brain metastases, Lung cancer, Screening.

Article History	Received: October 23, 2023	Revised: January 22, 2024	Accepted: January 29, 2024

1. INTRODUCTION

Lung cancer is one of the most common cancers worldwide, whose incidence and mortality make it a notable healthcare issue [1]. Metastatic tumors involving the brain are an important complication in the overall management of lung cancers, with an incidence of 17-57% [2, 3]. In fact, the median overall survival of brain metastases (BM) without treatment is <3 to 6 months [4]. Development of BM is devastating for patients, impairing neurological function and quality of life and indicating worse survival [5].

Detection and characterization of brain metastatic lesions, especially in number, location, size and viable tumor regions,

are of great importance for making therapeutic planning and evaluating the efficacy of treatment strategies. In the past, the two-dimensional (2D) contrast-enhanced T1-weighted imaging (CE T1WI) sequence or 2D post-contrast T1WI sequence was widely used at most institutions for detecting BM [6]. Metastatic lesion contrast on CE T1WI could be improved by administrating a high dose of contrast materials, suppressing the background signal with magnetization transfer (MT) techniques, or delaying imaging time [7 - 9]. Nonetheless, high-dose of contrast could increase false-positive or ambiguous findings, and the extra costs of contrast agents [10] and leptomeningeal metastases and small metastases located near the corticomedullary junction or vascular enhancement were not readily detected or conspicuous enough in 2D CE T1WI images even with high-dose of contrast or MT saturation [7, 8, 11, 12]. Also, delayed scanning was not fast and convenient enough. Currently, a three-dimensional(3D) CE T1WI sequence is recommended in a standardized brain tumor imaging protocol for BM (BTIP-BM) [13]. Although this will aid in accurately evaluating BM than 2D CE T1WI, especially small BM with diameter≤5mm, it's time-consuming and not friendly to some patients who couldn't tolerate longer scanning examination. Therefore, a quick, effective and budget-friendly method for detecting BM is required.

Fluid-attenuated inversion-recovery (FLAIR) is a heavily T2-weighted sequence which nulls cerebrospinal fluid (CSF) [14]. Due to a mild T1 weighting induced by the long inversion time, the contrast agents of gadolinium (Gd) could result in positive contrast enhancement in FLAIR imaging [11, 12]. The clinical utility of contrast-enhanced FLAIR (CE FLAIR) or post-contrast FLAIR sequence in a broad spectrum of intracranial pathological conditions has been shown in several studies, including brain tumors (gliomas, metastases, medulloblastoma *etc*.), leptomeningeal diseases, multiple sclerosis, traumatic brain injury, acute stroke and hyperglycemia-induced seizures [11, 12, 15 - 25]. Previous studies were mostly performed in limited patient groups and did not show more information on missed and misdiagnosed cases of BM on CE FLAIR for clinical reference [11, 12, 15]. The aim of this study is to explore the clinical utility of CE FLAIR and investigate a quick and efficient detecting method for BM of lung cancers by comparing the diagnostic potentials of CE T1WI, CE FLAIR and their combination.

2. MATERIALS AND METHODS

2.1. Patients

Two hundred and one consecutive patients (74 women, 127 men; mean age, 62 years; age range,26–81years) with primary lung cancers and clinical suspicion of BM were included and underwent baseline contrast-enhanced brain MRI (from May 2020 to May 2022). The distribution of the primary lung neoplasms (confirmed by cytology, biopsy or surgery) was as follows: adenocarcinoma(n=155), neuroendocrine carcinoma (n=31, small cell lung carcinoma=29, large cell neuroendocrine carcinoma=2), squamous cell carcinoma (n=11), adenosquamous carcinoma (n=2), sarcomatoid carcinoma (n=2). All the patients underwent follow-up MRIs within 6 months.

* Address correspondence to this author at the Department of Radiology, Shanghai Chest Hospital, School of Medicine, Shanghai Jiao Tong University, Building 1, Room 310, No. 241 Huaihai West Road, Shanghai, 200030, PR China;
E-mails: yuhongchest@163.com and augjuly@aliyun.com
#*These authors contributed equally to this work*

2.2. MRI Acquisitions

MR imaging was performed on a 3.0-T clinical MR imager (Prisma; SIEMENS Medical Systems; Erlangen, Germany). This study was approved by the Institutional Review Board of Shanghai Chest Hospital (No. KS23008), and informed consent was obtained from all patients for the MR study according to its guidelines. 2D fat-suppressed T1WI and fast FLAIR were performed before and after injection of gadopentetate dimeglumine, which was administered at the standard dose of 0.1 mmol/kg of body weight (single dose). The imaging acquisition workflow was as follows: axial T1WI (49 seconds) →axial FLAIR (48 seconds) →administration of contrast agents→ axial T2WI (29 seconds) →axial DWI (49 seconds) →axial, sagittal and coronal T1WI (two minutes and 59 seconds) →axial FLAIR (48 seconds). The imaging parameters for T1WI were 2050ms/24ms/1/256×256 (TR/TE/NEX/matrix), and those for FLAIR imaging were 8000ms/150ms/2200ms/1/150°/256×256 (TR/TE/TI/NEX/flip angle/matrix). All images were acquired with a section thickness of 5 mm, an intersection gap of 2 mm, field of view of 240mm. In the follow-up of the brain MRI, susceptibility-weighted imaging (SWI) was incorporated if a differential diagnosis was required. The imaging parameters for SWI were 27ms/19.7ms/15◦/ 140 Hz/320 × 240 × 52/3 mm/230 mm/0.72 mm × 0.72 mm × 2.5mm (TR/TE/flip angle/bandwidth/ matrix/slice thickness/ FOV/voxel size).

2.3. Image Analysis

Two experienced neuroradiologists who were blinded to clinical information and follow-up MR images reviewed the pre- and post-contrast images of T1WI (Group 1) and FLAIR (Group 2) on a workstation independently and determined possible abnormal contrast enhancement or abnormal signal intensity. A possible abnormally-enhanced lesion on CE T1WI or CE FLAIR was defined as a region that turned into hyperintense on post-contrast images compared to pre-contrast images. Possibly intrinsically high-signal-intensity areas, such as the choroid plexus, pituitary stalk and gland, and definite vascular structures(superior sagittal sinus, confluence of sinuses and straight sinus) were excluded. Leukoaraiosis and lacunar infarctions (shown on pre-contrast FLAIR but not enhanced on CE FLAIR) were excluded from the abnormal signal intensity. Furthermore, because these findings were too many to be counted, it could result the specificities of Group 2 being practically calculated. The abnormal findings were scored as 1 for metastatic and 0 for non-metastatic in the two groups. The diagnostic criteria for BM were as follows: (1) The round-like or irregular enhancement in parenchyma and ependyma with or without edema; (2) The enhancing curvilinear segments following the gyrus convolutions; (3) The enhancing skull lesions with expansive or non- expansive bone destruction. When disagreement existed, the third senior reviewer joined in to reach a consensus on the final judgement.

In the follow-up, MR images, cranial metastatic lesions

were finally confirmed by increase or decrease of lesion sizes/extents without or with chemotherapy or radiotherapy. Conversely, if the abnormal findings disappeared or didn't change in size/extent, they would be interpreted according to the overall consideration of the locations, imaging manifestations and medical histories. The differential diagnoses from BM as follows: (1) The lesions located near cerebral sulci and fissures, which were linear low-signal structures on SWI and whose sizes did not change on follow-up MR images, were considered as normal blood vessels; (2) The lesions located around cranial fossa, which were ambiguously contrast-enhanced on CE T1WI while not on CE FLAIR and disappeared on follow-up MR images, were considered as phase-shift artifacts; (3) The lesions which had patterns of caput medusae enhancement and whose extents did not change on follow-up MR images were considered as venous malformation; (4) The lesions located in the regions of brain parenchyma, which was enhanced on CE FLAIR while not on CE T1WI and improved by thrombolytic therapy, were considered as infarction-related lesions; (5) The lesions located in the regions of cerebral convexity, skull base, falx and tentorium, which was dural-tail enhanced both on CE T1WI and CE FLAIR and whose sizes didn't change, were considered as meningiomas; (6) The lesions located in skull, which was expansive, sharply demarcated and existed before lung cancer, were considered as cranial osteoma.

The number and locations of abnormally enhanced lesions/ abnormal signal intensity in Group 1 and Group 2 at initial diagnosis were recorded, and then the locations were classified as parenchyma and ependyma, leptomeninges and skull. The diameters of lesions located in parenchyma and ependyma were usually measured on CE T1WI, and edema conditions were documented. If the lesions were missed-diagnosed on CE T1WI, the diameters would be measured on CE FLAIR. The extension of the leptomeningeal metastases and the shapes of skull metastases in Group 1 and Group 2 were assessed. The features of false-negative (missed-diagnosed) and false-positive (misdiagnosed) lesions in Group 1 and Group 2 were analyzed and summarized.

2.4. Statistics

Interobserver reproducibility was assessed by calculating kappa statistics. The statistical differences between Group 1 and Group 2 were calculated using McNemar's test and Fisher's exact test. Predicted values of probabilities in Group 3 (combination of CE T1WI and CE FLAIR) were first calculated with the binary logistic regression model, and then receiver operating characteristic (ROC) analyses were conducted for Group 1, Group 2 and Group 3. The diagnostic confirmation stated above was used as the gold standard for ROC analysis. The areas under the receiver operating characteristic curve (AUC) from each group were compared with the DeLong method. A p-value < 0.05 was considered statistically significant. All statistical calculations were performed using statistics software (MedCalc, version 20.0.3).

3. RESULTS

3.1. Metastatic Findings

A total of 672 BMs in 149 of 201 patients were revealed. The cranial metastases were located in parenchyma (n=657) and ependyma(n=2), leptomeninges (n=6) and skull(n=7).

In 659 metastases of parenchyma and ependyma, 578 metastatic lesions were detected in Group 1, and 635 metastatic lesions in Group 2. The sizes of the metastatic lesions in the parenchymal and ependymal regions ranged from 2mm to 72mm. Two hundred and nineteen (33.2%) were ≤5 mm, 261 (39.6%) were 5–10 mm, 147 (22.3%) were 10–30 mm, and 32 (4.9%) were >30 mm. The sensitivities of metastatic lesions in parenchyma and ependyma (≤5 mm) in Group 1 and Group 2 were 77.6% and 92.7%, and there was a significant difference among them($p<0.0001$). The sensitivity of metastatic lesions (5-10 mm) in Group 2 was 97.7%, which was superior to 88.1% in Group 1 ($p<0.0001$). No statistical differences were observed in sensitivities of metastatic lesions (10-30 mm and >30 mm) between Group 1 and Group 2. It indicated that CE FLAIR had better performance than CE T1WI in detecting small BMs (≤10 mm). In the areas of parenchyma and ependyma, edema surrounding metastases and mass effects were absent in 81 false-negative cases in Group 1 and 20 false-negative cases in Group 2 (the other 4 false-negative cases in Group 2 were covered by edema areas) on account of their small sizes(≤10mm).

In 6 cases of leptomeningeal metastases, images in Group 1 showed only 3, while those in Group 2 showed all. Furthermore, the extent of 3 cases of leptomeningeal metastases shown on CE FLAIR were larger than those on CE T1WI.

In 7 cases of skull metastases, 4 lesions were revealed both in Group 1 and Group 2, which were easily seen due to expansive bone destructions. 3 non-expansive skull lesions were easily recognized in Group 2 while missed in Group 1.

3.2. Nonmetastatic Findings

According to clinical histories and comparison of the past, baseline and follow-up MR images, 42 abnormal findings were considered nonmetastatic, which included normal blood vessel enhancement(n=25), artifacts around cranial fossa (n=6), venous malformation(n=4), infarction-related lesions (n=3), meningiomas(n=3), and cranial osteoma (n=1). In the nonmetastatic findings, 25 normal vessel enhancements were all located near sulci and fissures, and their diameters were≤ 5 mm, the diameters of artifacts around the cranial fossa (6 cases) were ≤10mm and the average diameter of 3 meningiomas was 25.12±7.86mm. Diameter measurement was not suitable for other non-metastatic findings.

Interobserver reproducibility was substantial for Group 1 ($\kappa = 0.81$ [95% CI: 0.74, 0.87]) and Group 2 ($\kappa = 0.82$ [95% CI: 0.76, 0.89]). Both of Group 1 and Group 2 detected the majority of these metastatic lesions. The sensitivity of Group 2 was 96.4%, which was superior to that of Group 1 (87.1%) ($p<0.0001$). The specificities of Group 1 and Group 2 were 57.1% and 61.9%, and there was no significant difference among them($p=0.0755$). The distributions of false-negative and false-positive lesions in Group 1 and Group 2 were summarized in Tables **1** - **4**. Meanwhile, the illustrative images of false-negative and false-positive cases in the two groups were presented in Figs. (**1** and **2**).

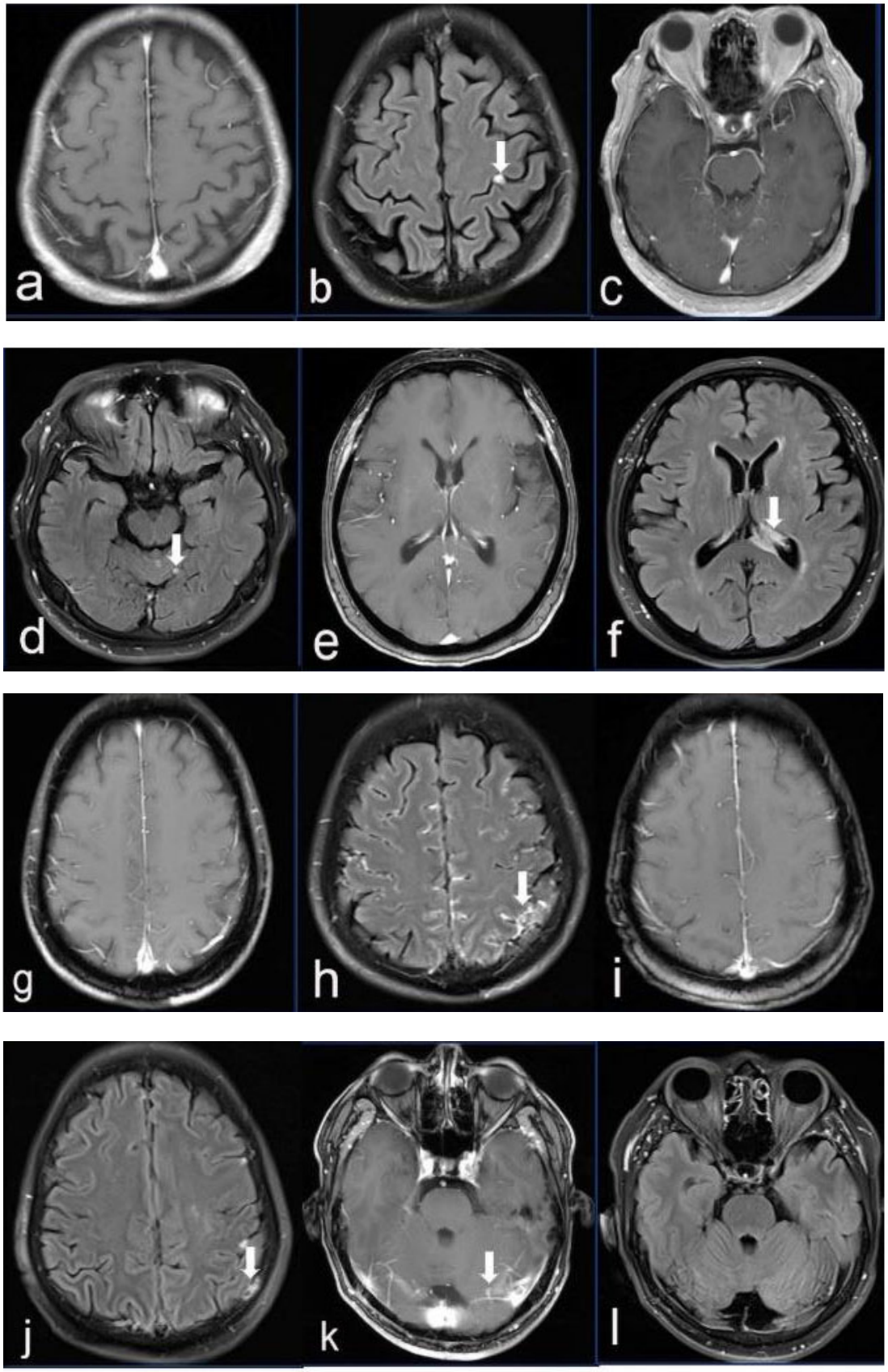

Fig. 1 contd.....

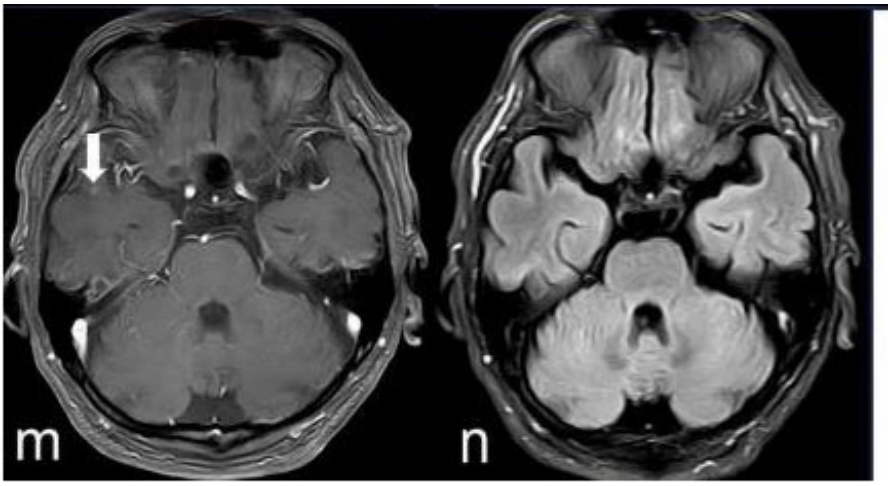

Fig. (1). The illustrative images of the false-negative (**a-j**) and false-positive (**k-n**) lesions in Group 1 compared with those on CE FLAIR. (**a-b**). A metastasis near the left central sulcus was markedly hyperintense on CE FLAIR (arrow, B) while missed on CE T1WI (**a**). (**c-d**). A metastasis near the tentorium was significantly enhanced on CE FLAIR (arrow, D) while missed in Group 1 (**c**). (**e-f**). An ependymal metastasis was easily recognized on CE FLAIR (arrow, F) while missed in Group 1 (**e**). **g-h**. Diffuse Lepto-meningeal metastases were shown on CE FLAIR (arrow, H) while not shown in Group 1 (**g**). (**i-j**). The non-enlarged metastasis in the left parietal bone was missed in Group 1 (**i**) while easily recognized on CE FLAIR (arrow, J). (**k-l**). A significantly enhanced lesion near sulcus and fissure in Group 1 (arrow, K) was confirmed as normal vessel structure by SWI (not shown here),while not interpreted as metastatic CE FLAIR (**l**). **m-n**. An abnormally-enhanced finding near the right middle fossa (arrow, M) was confirmed as an artifact, while not shown CE FLAIR (**n**).

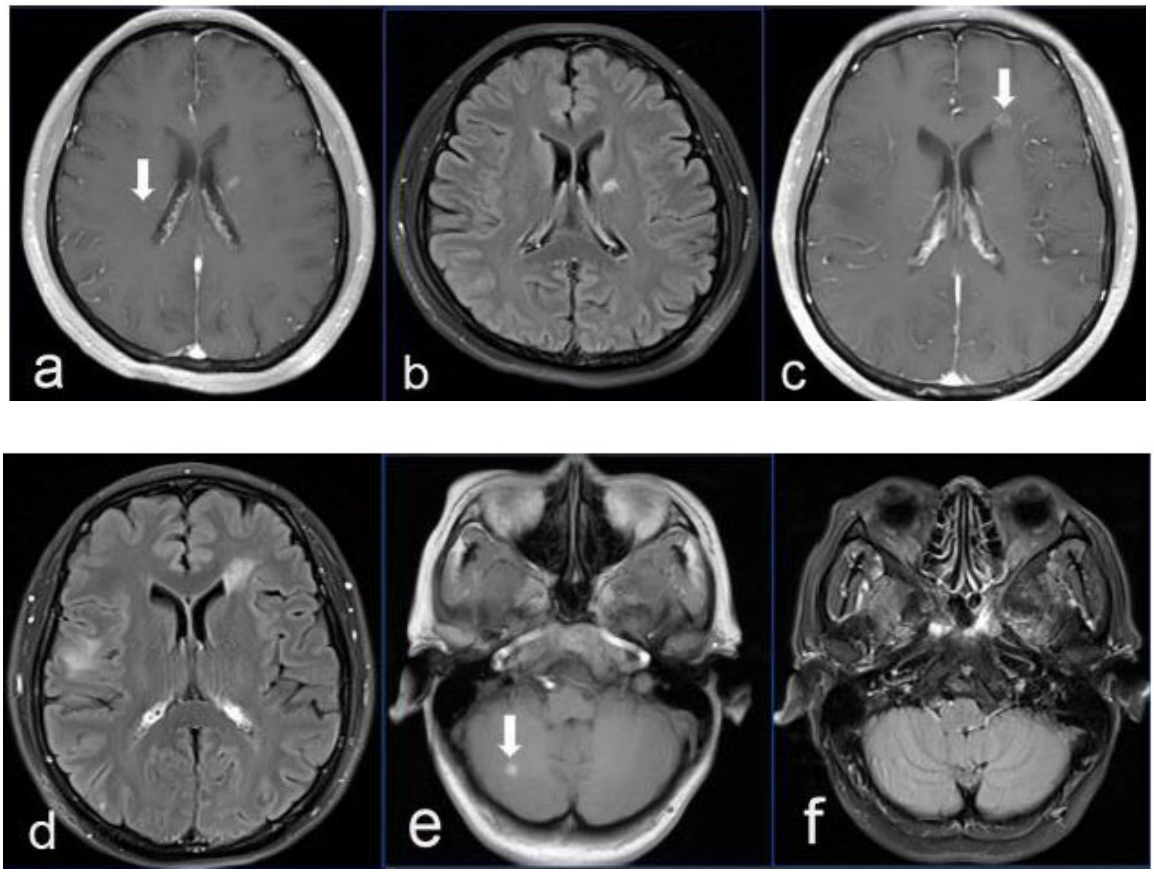

Fig. 2 contd.....

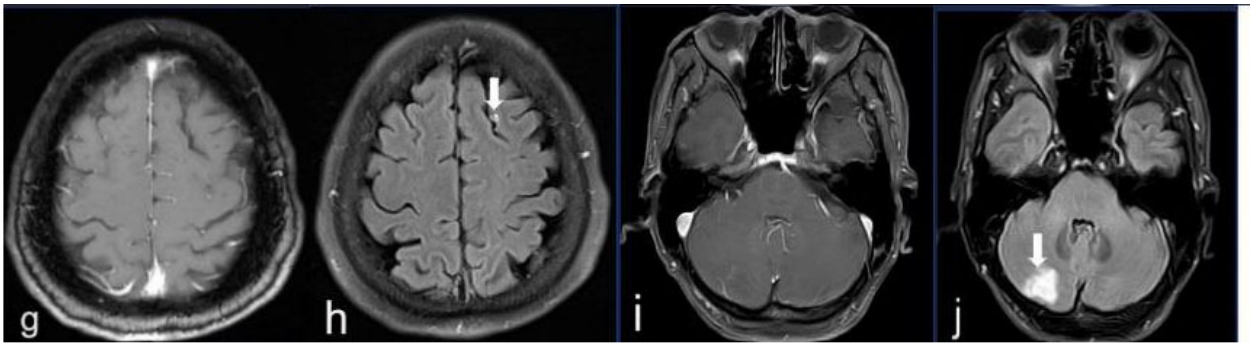

Fig. (2). The illustrative images of the false-negative (**a-f**) and false-positive (**g-j**) lesions in Group 2 compared with those on CE T1W or pre-contrast T1WI. (**a-b**). A metastasis in the right basal region was missed on CE FLAIR (**b**) while enhanced on CE T1WI (arrow, A). (**c-d**). A metastasis near the left ventricle was covered by edema in Group 2 (**d**) while enhanced on CE T1WI (arrow, C). (**e-f**). A metastasis with subacute hemorrhage was hyperintense and easily seen on pre-contrast T1WI (arrow, E) while missed in Group 2 (**f**). (**g-h**). A significantly enhanced finding near the left superior frontal sulcus in Group 2 (arrow, H) was confirmed as normal vessel structure by SWI (not shown), while not recognized as an abnormal enhancement on CE T1WI. (**i-j**). An enhanced lesion of the right cerebellar hemisphere, which was confirmed as acute infarction by DWI (not shown), was misdiagnosed as metastatic (arrow, J), whereas it wasn't abnormally-enhanced on CE T1WI (**i**).

Table 1. The distribution of false-negative lesions in Group 1 (pre and post T1WI).

Location and Features	Number
Cerebral cortex near sulci and fissures, diameter≤10 mm	57
Region around cerebral falx and tentorium, diameter≤5 mm	23
Ependyma, diameter=18mm	1
Lepto-meningeal location	3
None-expansive skull lesions	3

Table 2. The distribution of false-positive lesions in Group 1 (pre and post T1WI).

Location and Features	Number
Vessel enhancement near sulci and fissures, diameter≤5 mm	12
Artifacts around cranial fossa, diameter≤10 mm	6

Table 3. The distribution of false-negative lesions in Group 2 (pre and post FLAIR).

Location and Features	Number
Around lateral ventricles and basal region, diameter≤5 mm	16
Covered by edema areas, diameter≤30 mm	4
With subacute hemorrhage, diameter≤10 mm	4

Table 4. The distribution of false-positive lesions in Group 2 (pre and post FLAIR).

Location and Features	Number
Vessel enhancement near sulci and fissures, diameter≤5 mm	13
Enhancement after infarction	3

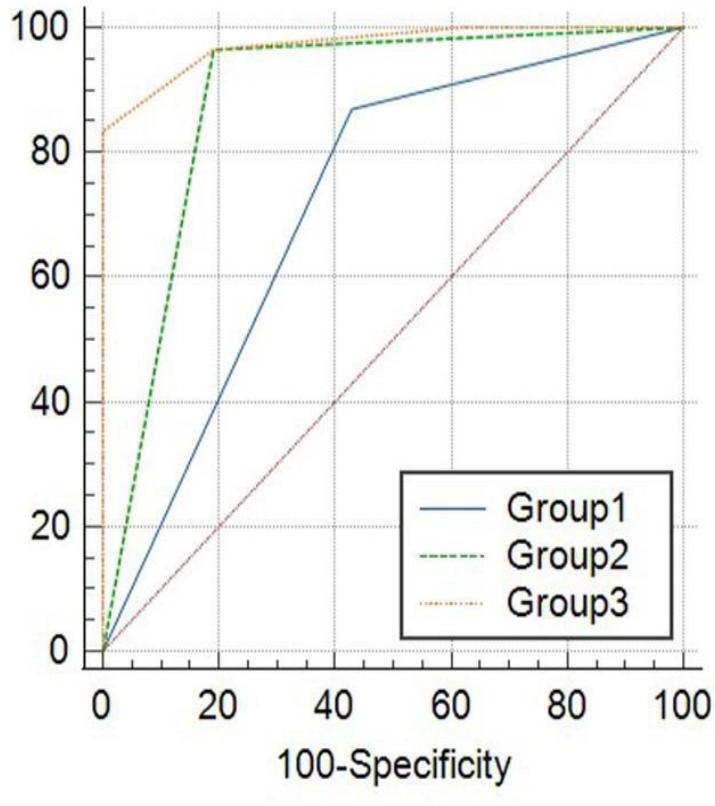

Fig. (3). Receiver operating characteristic (ROC) curves of Group 1, Group 2 and Group 3 (combination of CE FLAIR and CE T1WI) for the detection of cerebral metastases. Areas under ROC curves of Group 1, Group 2 and Group 3 are 0.720,0.887 and 0.973, respectively.

3.3. ROC Analysis

The ROC curves of Group 1, Group 2 and Group 3 are shown in Fig. (**3**). The AUC for the three groups were 0.720, 0.887 and 0.973, respectively. The area value under the ROC curve in Group 3 was significantly larger than that in Group 1 ($p<0.0001$)and Group 2 ($p=0.0006$). This demonstrated that the diagnostic confidence in Group 1(pre and post T1WI) was improved by the addition of CE FLAIR, and their combination provided a more effective way to detect cranial metastases on MRI examinations.

4. DISCUSSION

Images on CE FLAIR with long repetition show positive contrast enhancement in the majority of lesions, which are enhanced on T1-weighted images. The differences in enhancement features between CE T1WI and CE FLAIR images can be explained by a combination of a different T1-shortening effect at a certain concentration of Gd and a different T2 effect according to the vascularity of a lesion [25]. According to Dr. Mathews and his colleagues' phantom data graph [11], at lower concentrations of Gd, the FLAIR sequence was more sensitive to T1 shortening than CE T1WI and pathologic lesions on CE FLAIR might be conspicuous; at higher Gd concentrations, the FLAIR sequence was sensitive to T2 effects and pathologic lesions on CE FLAIR might be inconspicuous, whereas the lesions had better enhancement on CE T1WI. It has been reported that under the same achieved high signal intensity, only a quarter of the concentration of gadolinium-based contrast agent was required for CE FLAIR compared with CE T1WI [26]. It meant that the vague enhancing lesions on CE T1WI at lower concentrations of Gd might be more clearly enhanced on CE FLAIR. Hence, some investigators suggested the CE FLAIR imaging modality could be implemented to improve clinical MRI workflows for cancer patients [11, 12, 15, 25, 27].

The minimum standard of BTIP-BM consists of pre-contrast 3D T1WI, 2D T1WI, 2D FLAIR, 2D DWI, 2D T2WI, post-contrast 2D T1WI and 3D T1WI, which usually costs about 13 minutes and 34 seconds at least in our center without counting the time of contrast injection. In our study, the scanning sequences were adjusted (shown in methods and materials) in consideration of superior delayed enhancement on BM and influences of different Gd concentrations on enhancement between CE T1WI and CE FLAIR, and the whole protocol took 6 minutes and 52 seconds. In this new protocol, T2WI and DWI were adjusted after administration of Gd, which were slightly affected at lower concentrations of contrast agents [28, 29]. CE T1WI was delayed, and CE FLAIR was performed at last (4 minutes 17 seconds after Gd injection), which was assured to be conducted at lower concentrations of Gd for better observation [30]. Delayed enhancement did not affect the sensitivities of CE FLAIR [31, 32]. Therefore, this new protocol was relatively quick and convenient, which allowed for increased comfort for some patients who could not tolerate long-scanning examinations.

Our study indicated that the combination of CE FLAIR and

CE T1WI significantly improved diagnostic confidence in the detection of BM, compared with CE T1WI or CE FLAIR alone. This was attributable to the addition of CE FLAIR, which could lead to better visualization of parenchymal and ependymal (especially for small BMs≤10mm), lepto-meningeal and skull metastatic lesions. Dr. Terae S [27] also reported that the addition of postcontrast FLAIR imaging to pre- and postcontrast MT-T1WI significantly increased the confidence rating for metastases. On CE FLAIR, the contrast between lesions with adjacent CSF or white matter (lesion-to-background ratio) can be increased because the signal of CSF is nullified or the signal of white matter suppressed, even if the lesions are small. Besides, the signals of enhanced vascular structures (arteries, veins, and dural sinuses) that may mimic metastases or obscure metastatic lesions on CE T1WI are absent or minimized on CE FLAIR because CE FLAIR does not demonstrate contrast enhancement of blood vessels with the slow flow as does CE T1WI [12]. CE FLAR renders contrast-enhanced areas more conspicuously by preferentially suppressing the signals from normal brain parenchyma and vascular structures.

In parenchymal and ependymal metastatic lesions, our results indicated that CE T1WI had disadvantages in the demonstration of superficial and small enhancements (usually ≤10mm), and the false-negative metastatic lesions on CE T1WI were usually not markedly enhanced or confounded by vessel enhancement. However, CE FLAIR detected significantly more metastases than CE T1WI, especially for the lesions that were located near the corticomedullary junction or vascular enhancement, usually smaller than 10 mm and without mass effect or edema. Small BM are extremely important in clinics because they respond much better to therapies and can be controlled at a substantially higher rate, compared to larger lesions [33, 34]. Tsuchiya K *et al*. considered postcontrast FLAIR images as diagnostic potential equivalent to conventional postcontrast T1-weighted images [35]. In our research, CE FLAIR had a better detection efficacy, which was beneficial to therapeutic planning. Given its superior performance in distinguishing metastatic lesions from surrounding normal structures or edema, precontrast FLAIR might be omitted when CE FLAIR is acquired. Despite this, CE FLAIR alone could not entirely substitute CE T1WI. Firstly, some metastatic lesions around lateral ventricles and basal region, covered by edema, and with subacute hemorrhage (≤10 mm) were not enhanced on CE FLAIR, which led to false-negative results. Secondly, although CE FLAIR could minimize the enhancement of blood vessels and reduce phase-shift artifacts derived from vascular structures, some non-metastatic findings, such as vessel enhancements near sulci and fissures or in basal ganglia (≤5 mm), or infarction-related lesions were enhanced on CE FLAIR, which allowed mis-judgements of metastases and resulted in false positive findings. Except for the above cases, other cranial pathological lesions, such as glioblastoma or active multiple sclerosis, could be enhanced on CE FLAIR imaging [11, 12, 17, 21], which brought difficulties in the differential diagnosis between metastatic and non-metastatic lesions. Therefore, CE FLAIR alone has limited value in the assessment of cranial metastases and could be used as a supplementary sequence for the routine MRI protocol. Hence, we tried to combine CE T1WI and CE FLAIR, and the new MRI modality could be recommended for screening and diagnosis in patients with known malignancies and suspected BMs.

In lepto-meningeal metastatic lesions, our results demonstrated more metastases on CE FLAIR than on CE T1WI. Delayed post-contrast FLAIR imaging seemed to improve the diagnosis of lepto-meningeal carcinomatosis as compared to delayed post-contrast T1WI. The extents of 3 cases shown on CE FLAIR were larger than those on CE TIWI (Fig. **4**). This might be attributed to the confounding effects of enhanced vascular structures with lepto-meningeal metastases on CE T1WI and contrast leakage.

In skull metastases, three false-negative lesions on CE T1WI were restricted to cranial diploe and non-expansive, which resulted in omissions. Furthermore, due to suppression of signal intensity from surrounding tissues, they were conspicuous and clearly visualized on CE FLAIR.

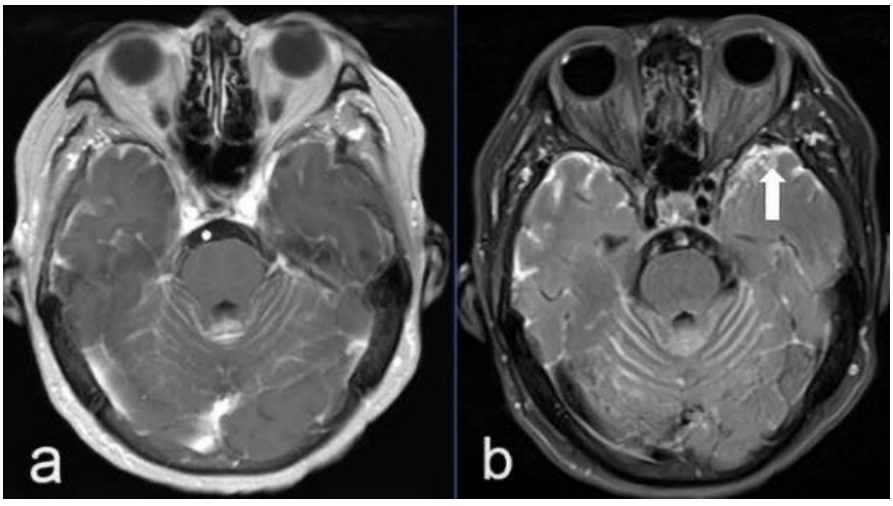

Fig. (4). (**A**) The extension of leptomeningeal metastases on CE FLAIR (arrow, **B**) was larger than that on CE T1WI.

There are several limitations in our study. (1) The study was conducted at a single medical center that mainly treats patients with lung cancer, and this would limit the generalizability of the findings, as different centers might have varying levels of expertise or equipment and other types of cancers. (2) 2D axial FLAIR (48 seconds) was adopted rather than 3D FLAIR (3 minutes and 24 seconds) for time-saving in our study. 3D FLAIR images are superior to 2D images in spatial resolution, which allows for a higher detection rate of small metastases (≤5mm) [31, 32]. Therefore, the protocol in our study was suggested for screening in some patients who could not tolerate longer scanning examinations and would take accurate evaluations before stereotactic radiotherapy (3) Most patients in this study would not like to take invasive pathological examinations of cranial lesions, so confirmation of BM in this study relied mainly on histories and follow-ups. However, the pathological confirmation of metastasis after surgical excision or stereotactic biopsy of the lesion would be more confirmatory of the nature of the lesions.

CONCLUSION

In conclusion, the delayed addition of CE FLAIR is recommended to be incorporated into conventional MRI scanning for patients with known malignancies and clinically suspected BMs, and the combination of CE T1WI and CE FLAIR can be rapid and effective for screening BM.

LIST OF ABBREVIATIONS

CE FLAIR	=	Contrast-enhanced Fast Fluid-attenuated Inversion Recovery
CE T1WI	=	Contrast-enhanced T1 Weighted Imaging
BM	=	Brain Metastases
2D	=	Two-dimensional
MT	=	Magnetization Transfer
3D	=	Three-dimensional
BTIP-BM	=	A Standardized Brain Tumor Imaging Protocol For BM
CSF	=	Cerebrospinal Fluid
Gd	=	Gadolinium
SWI	=	Susceptibility Weighted Imaging
ROC	=	Receiver Operating Characteristic
AUC	=	Areas under the Receiver Operating Characteristic Curve

ETHICS APPROVAL AND CONSENT TO PARTICIPATE

This study was approved by the Institutional Review Board of Shanghai Chest Hospital (No. KS23008).

HUMAN AND ANIMAL RIGHTS

No animals were used in this research. All procedures performed in studies involving human participants were in accordance with the ethical standards of institutional and/or research committee and with the 1975 Declaration of Helsinki, as revised in 2013.

STANDARDS OF REPORTING

STROBE guidelines were followed.

CONSENT FOR PUBLICATION

Informed consent was obtained from all patients for the MR study according to its guidelines

DATA AVAILABILITY STATEMENT

The datasets analyzed in this study are available from the correspondings authors [L.Z] and [H.Y] on reasonable request.

FUNDING

This study was supported by grants from the Interdisciplinary Program of Shanghai Jiaotong University (No. YG2021QN123).

CONFLICT OF INTEREST

The authors declare that they have no competing interests.

ACKNOWLEDGEMENTS

We thank Ms. Mengxiao Liu and Mr. Lude Cheng from MR Scientific Marketing, Customer Service, Siemens Healthcare Digital Technology Ltd for the debugging of MRI sequences.

REFERENCES

[1] Bray F, Ferlay J, Soerjomataram I, Siegel RL, Torre LA, Jemal A. Global cancer statistics 2018: GLOBOCAN estimates of incidence and mortality worldwide for 36 cancers in 185 countries. CA Cancer J Clin 2018; 68(6): 394-424. [http://dx.doi.org/10.3322/caac.21492] [PMID: 30207593]

[2] Robnett TJ, Machtay M, Stevenson JP, Algazy KM, Hahn SM. Factors affecting the risk of brain metastases after definitive chemoradiation for locally advanced non-small-cell lung carcinoma. J Clin Oncol 2001; 19(5): 1344-9. [http://dx.doi.org/10.1200/JCO.2001.19.5.1344] [PMID: 11230477]

[3] Sperduto PW, Yang TJ, Beal K, *et al.* Estimating survival in patients with lung cancer and brain metastases. JAMA Oncol 2017; 3(6): 827-31. [http://dx.doi.org/10.1001/jamaoncol.2016.3834] [PMID: 27892978]

[4] Lutterbach J, Bartelt S, Ostertag C. Long-term survival in patients with brain metastases. J Cancer Res Clin Oncol 2002; 128(8): 417-25. [http://dx.doi.org/10.1007/s00432-002-0354-1] [PMID: 12200598]

[5] Addeo R, De Rosa C, Faiola V, *et al.* Phase 2 trial of temozolomide using protracted low-dose and whole-brain radiotherapy for nonsmall cell lung cancer and breast cancer patients with brain metastases. Cancer 2008; 113(9): 2524-31. [http://dx.doi.org/10.1002/cncr.23859] [PMID: 18798231]

[6] Russell EJ, Geremia GK, Johnson CE, *et al.* Multiple cerebral metastases: Detectability with Gd-DTPA-enhanced MR imaging. Radiology 1987; 165(3): 609-17. [http://dx.doi.org/10.1148/radiology.165.3.3317495] [PMID: 3317495]

[7] Yuh WTC, Engelken JD, Muhonen MG, Mayr NA, Fisher DJ, Ehrhardt JC. Experience with high-dose gadolinium MR imaging in the evaluation of brain metastases. AJNR Am J Neuroradiol 1992; 13(1): 335-45. [PMID: 1595472]

[8] Yuh WTC, Tali ET, Nguyen HD, Simonson TM, Mayr NA, Fisher DJ. The effect of contrast dose, imaging time, and lesion size in the MR detection of intracerebral metastasis. AJNR Am J Neuroradiol 1995; 16(2): 373-80. [PMID: 7726087]

[9] Schörner W, Laniado M, Niendorf HP, Schubert C, Felix R. Time-dependent changes in image contrast in brain tumors after gadolinium-DTPA. AJNR Am J Neuroradiol 1986; 7(6): 1013-20. [PMID: 3098065]

[10] Sze G, Johnson C, Kawamura Y, *et al.* Comparison of single- and triple-dose contrast material in the MR screening of brain metastases. AJNR Am J Neuroradiol 1998; 19(5): 821-8. [PMID: 9613494]

[11] Mathews VP, Caldemeyer KS, Lowe MJ, Greenspan SL, Weber DM, Ulmer JL. Brain: gadolinium-enhanced fast fluid-attenuated inversion-recovery MR imaging. Radiology 1999; 211(1): 257-63. [http://dx.doi.org/10.1148/radiology.211.1.r99mr25257] [PMID: 10189481]

[12] Essig M, Knopp MV, Schoenberg SO, *et al.* Cerebral gliomas and metastases: Assessment with contrast-enhanced fast fluid-attenuated inversion-recovery MR imaging. Radiology 1999; 210(2): 551-7. [http://dx.doi.org/10.1148/radiology.210.2.r99ja22551] [PMID: 10207443]

[13] Kaufmann TJ, Smits M, Boxerman J, *et al.* Consensus recommendations for a standardized brain tumor imaging protocol for clinical trials in brain metastases. Neuro-oncol 2020; 22(6): 757-72. [http://dx.doi.org/10.1093/neuonc/noaa030] [PMID: 32048719]

[14] Rydberg JN, Hammond CA, Grimm RC, *et al.* Initial clinical experience in MR imaging of the brain with a fast fluid-attenuated inversion-recovery pulse sequence. Radiology 1994; 193(1): 173-80. [http://dx.doi.org/10.1148/radiology.193.1.8090888] [PMID: 8090888]

[15] Ercan N, Gultekin S, Celik H, Tali TE, Oner YA, Erbas G. Diagnostic value of contrast-enhanced fluid-attenuated inversion recovery MR imaging of intracranial metastases. AJNR Am J Neuroradiol 2004; 25(5): 761-5. [PMID: 15140715]

[16] Goo HW, Choi CG. Post-contrast FLAIR MR imaging of the brain in children: Normal and abnormal intracranial enhancement. Pediatr Radiol 2003; 33(12): 843-9. [http://dx.doi.org/10.1007/s00247-003-1057-8] [PMID: 14551756]

[17] Absinta M, Vuolo L, Rao A, *et al.* Gadolinium-based MRI characterization of leptomeningeal inflammation in multiple sclerosis. Neurology 2015; 85(1): 18-28. [http://dx.doi.org/10.1212/WNL.0000000000001587] [PMID: 25888557]

[18] Ueda F, Okuda M, Aburano H, Yoshie Y, Matsui O, Gabata T. Cranial pachymeningeal involvement in POEMS syndrome: Evaluation by pre- and post-contrast FLAIR and T₁-weighted Imaging. Magn Reson Med Sci 2017; 16(3): 231-7. [http://dx.doi.org/10.2463/mrms.mp.2015-0014] [PMID: 28003622]

[19] Parmar H, Sitoh YY, Anand P, Chua V, Hui F. Contrast-enhanced flair imaging in the evaluation of infectious leptomeningeal diseases. Eur J Radiol 2006; 58(1): 89-95. [http://dx.doi.org/10.1016/j.ejrad.2005.11.012] [PMID: 16386866]

[20] Galassi W, Phuttharak W, Hesselink JR, Healy JF, Dietrich RB, Imbesi SG. Intracranial meningeal disease: Comparison of contrast-enhanced MR imaging with fluid-attenuated inversion recovery and fat-suppressed T1-weighted sequences. AJNR Am J Neuroradiol 2005; 26(3): 553-9. [PMID: 15760865]

[21] Bagheri MH, Meshksar A, Nabavizadeh SA, Borhani-Haghighi A, Ashjazadeh N, Nikseresht AR. Diagnostic value of contrast-enhanced fluid-attenuated inversion-recovery and delayed contrast-enhanced brain MRI in multiple sclerosis. Acad Radiol 2008; 15(1): 15-23. [http://dx.doi.org/10.1016/j.acra.2007.07.022] [PMID: 18078903]

[22] Kim SC, Park SW, Ryoo I, *et al.* Contrast-enhanced FLAIR (fluid-attenuated inversion recovery) for evaluating mild traumatic brain injury. PLoS One 2014; 9(7): e102229. [http://dx.doi.org/10.1371/journal.pone.0102229] [PMID: 25028975]

[23] Lee KM, Kim JH, Kim E, Choi BS, Bae YJ, Bae HJ. Early stage of hyperintense **acute reperfusion marker on contrast-enhanced FLAIR images in patients with acute stroke.** AJR Am J Roentgenol 2016; 206(6): 1272-5. [http://dx.doi.org/10.2214/AJR.15.14857] [PMID: 27010867]

[24] Lee EJ, Kim KK, Lee EK, Lee JE. Characteristic MRI findings in hyperglycaemia-induced seizures: diagnostic value of contrast-enhanced fluid-attenuated inversion recovery imaging. Clin Radiol 2016; 71(12): 1240-7. [http://dx.doi.org/10.1016/j.crad.2016.05.006] [PMID: 27289324]

[25] Lee EK, Lee EJ, Kim S, Lee YS. Importance of contrast-enhanced fluid-attenuated inversion recovery magnetic resonance imaging in various intracranial pathologic condition. Korean J Radiol 2016; 17(1): 127-41. [http://dx.doi.org/10.3348/kjr.2016.17.1.127] [PMID: 26798225]

[26] Oguz KK, Cila A. Rim enhancement of meningiomas on fast FLAIR imaging. Neuroradiology 2003; 45(2): 78-81. [http://dx.doi.org/10.1007/s00234-002-0914-8] [PMID: 12592487]

[27] Terae S, Yoshida D, Kudo K, Tha KK, Fujino M, Miyasaka K. Contrast-enhanced FLAIR imaging in combination with pre- and postcontrast magnetization transfer T1-weighted imaging: Usefulness in the evaluation of brain metastases. J Magn Reson Imaging 2007; 25(3): 479-87. [http://dx.doi.org/10.1002/jmri.20847] [PMID: 17326092]

[28] Fırat AK, Şanlı B, Karakaş HM, Erdem G. The effect of intravenous gadolinium-DTPA on diffusion-weighted imaging. Neuroradiology 2006; 48(7): 465-70. [http://dx.doi.org/10.1007/s00234-006-0091-2] [PMID: 16673073]

[29] Yamada K, Kubota H, Kizu O, *et al.* Effect of intravenous gadolinium-DTPA on diffusion-weighted images: Evaluation of normal brain and infarcts. Stroke 2002; 33(7): 1799-802. [http://dx.doi.org/10.1161/01.STR.0000020355.29423.61] [PMID: 12105356]

[30] Jin T, Ge M, Huang R, *et al.* Utility of contrast-enhanced T2 FLAIR for imaging brain metastases using a half-dose high-relaxivity contrast agent. AJNR Am J Neuroradiol 2021; 42(3): 457-63. [http://dx.doi.org/10.3174/ajnr.A6931] [PMID: 33361381]

[31] Chen W, Wang L, Zhu W, *et al.* Multicontrast single-slab 3D MRI to detect cerebral metastasis. AJR Am J Roentgenol 2012; 198(1): 27-32. [http://dx.doi.org/10.2214/AJR.11.7030] [PMID: 22194476]

[32] Ahn SJ, Chung TS, Chang JH, Lee SK. The added value of double dose gadolinium enhanced 3D T2 fluid-attenuated inversion recovery for evaluating small brain metastases. Yonsei Med J 2014; 55(5): 1231-7. [http://dx.doi.org/10.3349/ymj.2014.55.5.1231] [PMID: 25048479]

[33] Chang EL, Hassenbusch SJ III, Shiu AS, *et al.* The role of tumor size in the radiosurgical management of patients with ambiguous brain metastases. Neurosurgery 2003; 53(2): 272-81. [http://dx.doi.org/10.1227/01.NEU.0000073546.61154.9A] [PMID: 12925241]

[34] Ranjan T, Abrey LE. Current management of metastatic brain disease. Neurotherapeutics 2009; 6(3): 598-603. [http://dx.doi.org/10.1016/j.nurt.2009.04.012] [PMID: 19560748]

[35] Tsuchiya K, Katase S, Yoshino A, Hachiya J. Pre- and postcontrast FLAIR MR imaging in the diagnosis of intracranial meningeal pathology. Radiat Med 2000; 18(6): 363-8. [PMID: 11153689]